Determining Lignin Degradation in White-Rot Fungi-Treated *Sacrau* Poplar: Lignin Structural Changes and Degradation Compound Analysis

Liming Zhang, Tingting You, Tian Zhou, Lu Zhang, and Feng Xu *

Determining the structural changes of lignin during bio-treatment will facilitate the understanding of biomass recalcitrance during the sustainable production of chemicals and fuels. However, the analysis of milled wood lignin (MWL) cannot completely elucidate the complex and irregular structural changes therein. In this study, MWL and lignin degradation compounds were extracted from white-rot fungi-treated poplar in order to unveil the degradation process. Results from MWL revealed that the cleavage of β-O-4′ linkages (from 76.4/100Ar to 31.5/100Ar) and the degradation of β–β′ and β-5′ linkages clearly occurred, resulting in a decrease in molecular weight. In addition, G-type lignin was more degraded than S-type lignin, with a slightly elevated S/G ratio from 1.13 to 1.29. Further analyses of lignin degradation compounds confirmed these results by showing a high amount of conjugated and unconjugated C=O functionalities. Furthermore, the degradation product of G-type lignin (vanillin) was detected by 2D HSQC NMR and GC-MS. This study of lignin alterations during white-rot fungi treatment could be beneficial for the sustainable production of chemicals, materials, and fuels from renewable plant resources.

Keywords: White-rot fungi; Lignin; Enzyme activity; 2D HSQC NMR; Degradation compounds

*Contact information: Beijing Key Laboratory of Lignocellulosic Chemistry, Beijing Forestry University, Beijing, 100083, China; *Corresponding author: xfx315@bjfu.edu.cn*

INTRODUCTION

Most terrestrial biomass (including tree trunks and grass stems) is sequestered in lignocellulosic macrostructures that are composed of cellulose, hemicelluloses, and lignin (Yelle *et al.* 2011). Lignin is recalcitrant to hydrolytic depolymerization because it is a combinatorial and racemic polymer of phenylpropanoid subunits connected *via* ether and carbon-carbon bonds (Zhao and Dixon 2011), which protects plant structural polysaccharides against microbial attack. White-rot fungi are the only organisms capable of degrading (mineralizing) lignin in wood, thus opening up the plant cell wall (Martínez *et al.* 2011). With the development of lignocellulose biorefineries, the question of how white-rot fungi circumvent wood and remove lignin has drawn attention because of the demand for the sustainable production of chemicals, materials, and fuels from renewable plant resources (Bozell *et al.* 2011; Wörmeyer *et al.* 2011).

Lignin can be oxidized and degraded by a ligninolytic system generated by white-rot fungi, which is composed of lignin peroxidase (LiP), Mn-oxidizing peroxidases, manganese peroxidase, and laccase (Umezawa and Higuchi 1987; Heinfling *et al.* 1998; Elegir *et al.* 2005; Mate *et al.* 2013). Early research on the utilization of white-rot fungi for improving degradation mainly focused on the utilization of a specific number of fungal species and strains. Zadrazil (1985) examined approximately 200 strains of white-rot fungi

and found that *Phanerochaete chrysosporium*, *Cyathus stercoreus*, and *Pleurotus spp*. were most commonly used. However, the mechanism of cleaved lignin structures in biodegraded wood attacked by white-rot fungi is poorly understood. In recent years, the mechanism by which lignin model compounds are degraded by the ligninolytic system has been studied (Elegir *et al.* 2005). Research on the reactivity of the ligninolytic system on lignin model compounds revealed that LiP attacks the β-O-4′ linkage of the lignin model (Umezawa *et al.* 1987) and that laccase oxidizes β-5′ and 5-5′ lignin substructures in the presence of phenolic groups (Elegir *et al.* 2005). Manganese peroxidase (MnP) oxidizes and depolymerizes natural and synthetic lignins as well as entire lignocelluloses (Hofrichter 2002). However, whether these mechanisms occur in the biological degradation process is unclear because of the complex macromolecular structure of lignin (a branched polymer comprised of different units and inter-unit bonds) and its intimate association with cell-wall polysaccharides.

The isolation of lignin from fungi-degraded lignocellulosic material is more intuitive than investigating lignin model compounds. However, elucidating the mechanisms of lignin macromolecule degradation or modification during bio-treatment is challenging because it is difficult to obtain a representative lignin sample. Milled wood lignin (MWL) is a representative source of native lignin and has been extensively used to determine the native lignin structure (Wen *et al.* 2013). However, the analysis of MWL cannot completely elucidate the complex and irregular structural changes of bio-treated samples, although the primary structure is well understood (Mao *et al.* 2013). The main reasons for this are: (1) isolated MWL is mainly extracted from the middle lamella, whereas biodegradation occurs in multiple locations (Wen *et al.* 2013), and (2) some "low-molecular" fractions are lost during separation and extraction. Thus, it is equally important to analyze the degradation products generated during white-rot fungi treatment.

In this study, *Sacrau* poplar was treated with the white-rot fungi *Trametes pubescens* C7571 and *Trametes versicolor* C6915 under solid-state conditions. The manganese peroxidase (MnP), lignin peroxidase (LiP), laccase, and hemicellulase activities were determined using a UV spectrophotometer; lignin structural changes (MWL and lignin degradation products) were characterized by Fourier translation infrared spectrum (FT-IR), two-dimensional ^{1}H-^{13}C NMR (2D HSQC NMR), and gas chromatography-mass spectrometer (GC-MS). This analysis enhances the understanding of structural changes that occur in bio-treated lignin.

EXPERIMENTAL

Fungal Incubation

Sacrau poplar was harvested from the experimental farm at Beijing Forestry University, Beijing, China. Before treatment, the wood sample was ground to pass through a 0.9-mm-sized screen. Two fungal strains, *T. pubescens* C7571 and *T. versicolor* C6915, were collected from Guangdong and Hebei provinces in China, respectively. Biological treatment was carried out in a 250-mL Erlenmeyer flask with 5 g of air-dried poplar wood and 12.5 mL of distilled water. The samples were sterilized in the autoclave for 20 min at 121 °C and inoculated with 5 mL of inoculum. The cultures were incubated statically at 28 °C for 4, 8, 12, and 16 weeks. The non-inoculated sample served as the control. All experiments were performed in triplicate.

Enzyme Assays

The enzymes were extracted with 50 mM sodium acetate buffer (pH 5.5) supplemented with Tween 60 (0.1 g/L). The entire contents of each bioreactor was transferred to an Erlenmeyer flask and extracted with 500 mL of extracting solution. Five successive extractions were performed at 120 rpm for 4 h at 10 ± 1 °C. After the second extraction, the wood chips were stored overnight while soaking in the extraction solution at 4 °C. The crude extracts were recovered by filtration through a fine filter paper (Souza-Cruz *et al.* 2004). Enzyme activities were determined at 25 °C using a Helios gamma UV-Vis spectrophotometer (Thermo Fischer Scientific, California, USA). Manganese peroxidase activity was determined according to the modified method of Heinfling *et al.* (1998) by the formation of Mn^{3+-} tartrate (ε238 = 6500 M/cm) from 0.10 mM $MnSO_4$ using 100 mM tartrate buffer (pH 5) and 0.10 mM H_2O_2. Lignin peroxidase activity was monitored at pH 3.0 according to Tien and Kirk (1988), and the formation of veratraldehyde was monitored at 310 nm (ε310 = 9.3 mM^{-1} cm^{-1}). Laccase was measured following the oxidation of 2.0 mM 2, 2′-azino-bis (3-ethylbenzthiazoline-6-sulphonic acid, ABTS) at 420 nm (Dias *et al.* 2004). Hemicellulase activity was measured according to Ghose and Bisaria (1987). The liberated reducing sugars were quantified using dinitrosalicylic acid (DNS) reagent (Miller 1959).

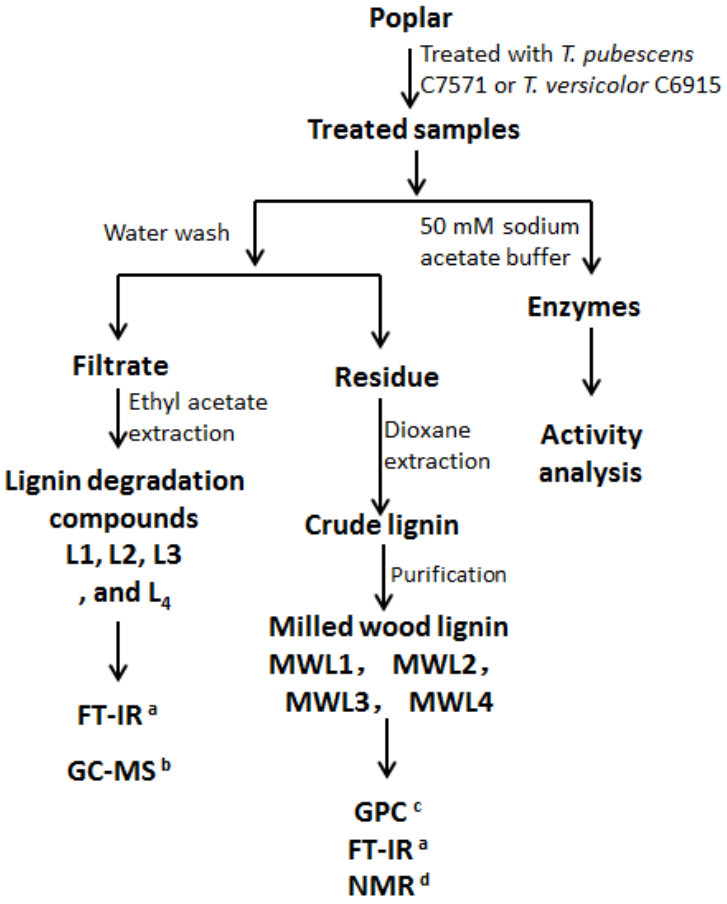

Fig. 1. Lignin isolation and enzyme activity analysis of bio-treated poplar
[a] FT-IR, Fourier translation infrared spectrum; [b] GC-MS, gas chromatography-mass spectrometer; [c] GPC, gel permeation chromatography; [d] NMR, nuclear magnetic resonance

Determination of Lignin

MWL was isolated and purified according to the method of Björkman (1954). MWL0 was lignin extracted from the untreated sample, and MWL1, MWL2, MWL3, and MWL4 were extracted from poplar treated with *T. pubescens* C7571 for 4 weeks, 8 weeks, 12 weeks, and 16 weeks, respectively. The lignin degradation products in these four bio-treated poplar samples were extracted with ethyl acetate and labeled L1, L2, L3, and L4 (Fig. 1). The weight average (M_w) and number-average (M_n) molecular weights of the lignin fractions were determined using gel permeation chromatography (GPC; Agilent 1200, California, USA). The sugar concentration in lignin was analyzed using a Dionex high-performance anion exchange chromatography (HPAEC) system (model ICS-3000, California, USA). FT-IR spectra of the lignin fractions were collected using a Thermo Scientific Nicolet iN10 FT-IR Microscope (Thermo Nicolet Corporation, Madison, WI, USA) equipped with a liquid nitrogen-cooled MCT detector. The dried fractions were ground and pelletized using KBr, and the spectra were recorded in the range of 4000 to 700 cm^{-1} at a 4-cm^{-1} resolution, with 128 scans per sample. Before data collection, background scanning was performed for correction. NMR spectra were recorded on a Bruker AVIII 400 MHz spectrometer (Saarbrucken, Germany) at 25 °C in DMSO-d6. Analytical Py-GC/MS of the lignin was performed using a CDS Pyroprobe 5200HP pyrolyzer (Chemical Data Systems, California, USA) connected to a Perkin Elmer GC/MS apparatus (Clarus 560, California, USA) equipped with an Elite-35MS capillary column (30 × 0.25 mm inner diameter, 0.25-μm film thickness). Compounds were identified by comparing their mass spectra with the NIST library (Wen *et a*l. 2014).

RESULTS AND DISCUSSION

Enzyme Activities

The enzyme activities of the fungi with different treatment times are presented in Fig. 2. The MnP activity of *T. pubescens* C7571 developed gradually over the treatment period, showing a maximum value of 0.60 U/mL during week 16. *T. versicolor* C6915 showed maximum MnP activity (0.43 U/mL) during week 4 and then declined, and it showed lower activity overall than *T. pubescens* C7571 (Fig. 2(a)). In the case of laccase activity (Fig. 2(b)), the more active producer was *T. versicolor* C6915, with a maximum value (2.23 U/mL) during week 12, while for *T. pubescens* C7571, the peak was observed at week 8 (0.69 U/mL). In contrast, LiP activity was higher for *T. pubescens* C7571 for all treatment times (Fig. 2(c)). Furthermore, ligninase activity was much higher than that of hemicellulase, and the hemicellulase of *T. pubescens* C7571 showed maximum activity during week 8 (0.03 U/mL), without obvious differences from the other treatment periods (Fig. 2(d)).

The production of ligninolytic enzymes during degradation by white-rot fungi has already been reported by several authors. Using a culture medium containing wheat straw incubated with fungi, Kapich *et al.* (2005) reported that *F. fomentarius* had an MnP activity value of 0.17 U/mL and *B. adusta* had a laccase activity value of 0.22 U/mL. More recently, Arora and Sharma (2010) presented values for laccase and MnP in *T. versicolor* of approximately 2.40 and 2.00 U/mL, respectively. The differing values reported in the literature were mainly because of the diversity of growth media and fungi strains.

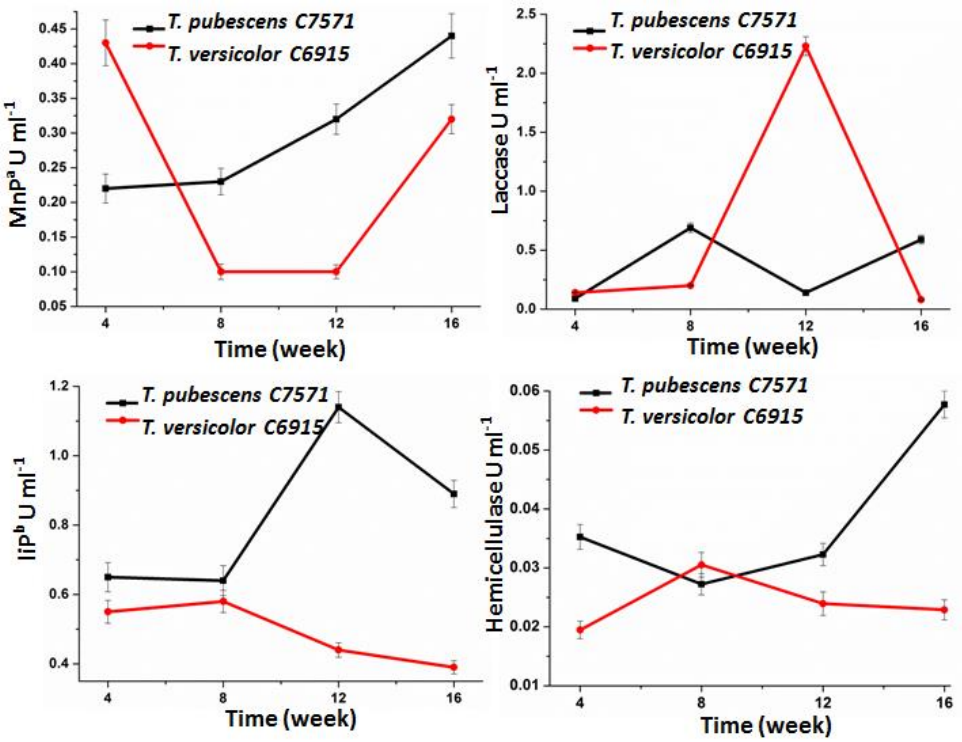

Fig. 2. Enzyme activities of white-rot fungi during the incubation period
[a] MnP, Manganese peroxidase; [b] LiP, lignin peroxidase

Lignin Component Changes

The decrease in lignin content differed between the two fungi-treated samples during different periods (Fig. 3). A lignin decrease of 6.6% (from 23.5% to 16.9%) and 5.1% (from 23.5% to 18.4%) was measured in the initial degradation period of *T. pubescens* C7571 and *T. versicolor* C6915, respectively. During this treatment period (week 4), LiP was the only enzyme whose activity was higher in *T. pubescens* C7571 than in *T. versicolor* C6915 (Fig. 2). This result was explained by the fact that LiP oxidizes non-phenolic lignin (Umezawa *et al.* 1987). Between week 4 and week 8, the decrease was approximately 2.7% for both types of white-rot fungi. Thus, there was a first phase (0 to 4 weeks) of growth, during which a rapid decrease in lignin was observed, and a second phase in which the values remained fairly stable. Additionally, during this treatment period, nearly all enzyme activity for *T. pubescens* C7571 was higher than that of *T. versicolor* C6915, except for that of hemicellulase. Hemicellulases are extremely important in the degradation of lignocellulosic biomass because of their lignin-carbohydrate complexes (LCCs) (Dinis *et al.* 2009). During week 16, *T. pubescens* C7571 showed higher activity for all three enzymes during the last treatment period (Fig. 2), thus yielding a low lignin content of 10.4%. A recent study also demonstrated the low enzyme producing capabilities of *T. versicolor* that laccase and MnP activity was only detectable and no LiP activity was detected (Kuhar et al. 2015). The results of enzyme activities as well as lignin component changes confirmed that the ability of *T. versicolor* to remove lignin was weaker than *T. pubescens* C7571. Chemical analyses in other studies have also indicated that this species is a non-selective type and that it removes all types of cell-wall constituents not only lignin (Bari et al. 2015). In summary, lignin degradation varied during different treatment periods; because *T. pubescens* C7571 showed a higher capacity for lignin degradation, it was considered for more specific studies.

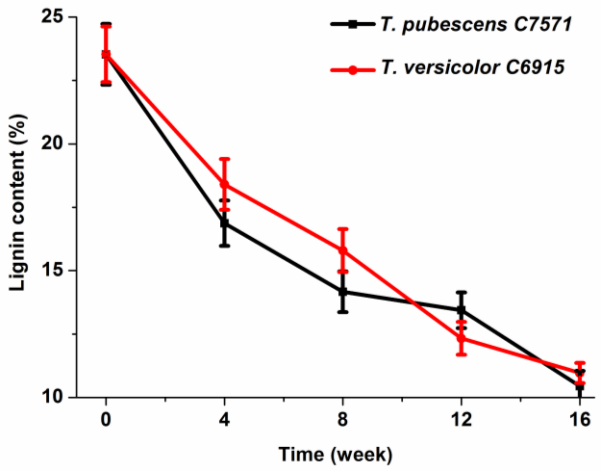

Fig. 3. Changes in lignin content during the incubation period

Chemical Component Analysis and Molecular Weight of Extracted Lignin

To reveal the effect of white-rot fungi treatment on the structural changes of lignin, MWL1, MWL2, MWL3, and MWL4 from *T. pubescens* C7571-treated poplar were further investigated. The sugar analysis of the extracted lignin fractions is listed in Table 1. The lignin fraction from the untreated sample had a relatively higher amount of sugar (6.49%) than the treated samples. Comparatively, MWL4 obtained from treated samples during the last 16 weeks had the lowest amount of bound sugars (0.97%). This result might be caused by the destruction of linkages between lignin and carbohydrates by the hemicellulase in white-rot fungi (Dinis *et al.* 2009). In all cases, xylose was the predominant sugar (0.28 to 3.06%), followed by mannose, glucose, and galactose, with a small amount of arabinose. An increase in treatment time from 4 to 16 weeks resulted in a noticeable decrease in xylose content (from 0.92% to 0.28%).

Table 1. Percentage of Neutral Sugars in the Isolated Lignin Fractions

Neutral Sugars (% of lignin sample, w/w)	Lignin Fraction				
	MWL0	MWL1	MWL2	MWL3	MWL4
Arabinose	0.09	0.13	0.31	ND[a]	ND[a]
Galactose	0.11	0.08	0.06	0.12	0.11
Glucose	0.65	0.55	0.16	0.28	0.26
Mannose	2.5	0.18	0.14	ND[a]	0.23
Xylose	3.06	0.92	0.39	0.44	0.28
Glucuronic Acid/Galacturonic Acid	0.08/0	0.61/0	0.77/0	0.43/0	0.09/0
Total	6.49	2.47	1.83	1.27	0.97

[a] ND, not detected

The molecular weight distribution of the extracted lignin samples was analyzed using gel permeation chromatography (GPC). Changes in the molecular weights of lignin provide insights to lignin fragmentation and re-condensation reactions during bio-treatment. As shown in Table 2, all lignin fractions possessed narrow molecular weight

distributions (M_w/M_n, lower than 1.5). The molecular weight of the MWL0 sample was M_w 3585.6 g/mol and M_n 2451.5 g/mol. When treated for 4 to 12 weeks, the extracted lignin had low molecular weights (2555.3 to 3226.4 g/mol and 1773.0 to 2250.0 g/mol). A significant reduction in molecular weight was observed in the lignin fraction MWL4 (M_w 2555.3 g/mol and M_n 1773.0 g/mol). The decrease in molecular weight indicated that lignin was fragmented during bio-treatment (discussed below).

Table 2. Weight-average (M_w), Number-average (M_n) Molecular Weights, and Polydispersity (M_w/M_n) of the Isolated Lignin Fractions

Lignin Fraction	M_w	M_n	M_w/M_n
MWL0	3585.6	2451.5	1.46
MWL1	3226.4	2250.0	1.43
MWL2	2887.2	2038.5	1.42
MWL3	3238.8	2468.1	1.31
MWL4	2555.3	1773.0	1.44

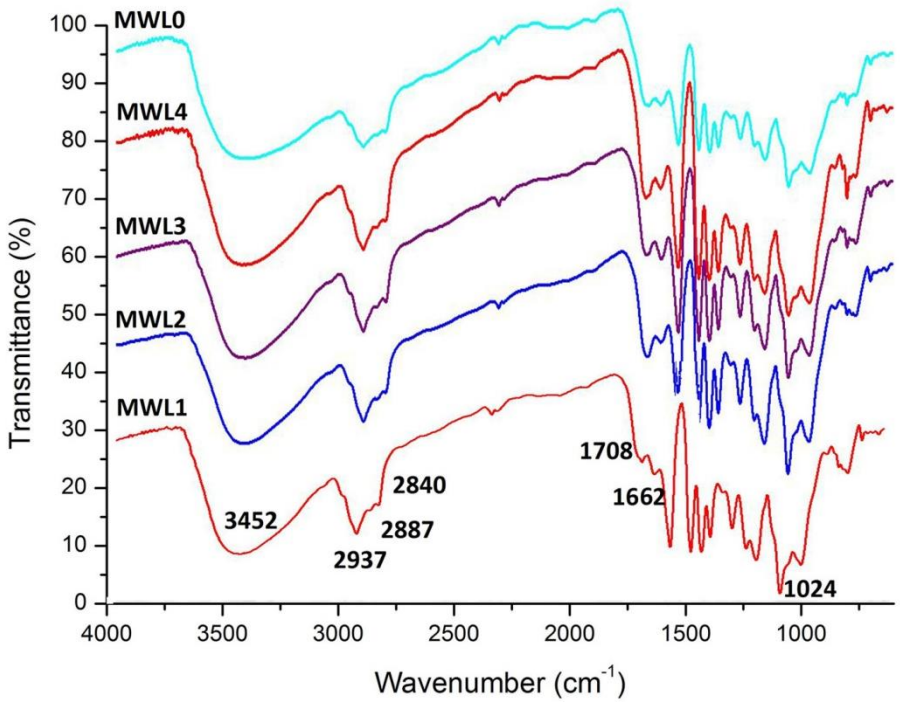

Fig. 4. FT-IR spectra of the extracted lignin fractions

FT-IR Spectra of the Extracted Lignin

To better understand lignin structural changes, the extracted lignin fractions were characterized by FT-IR spectroscopy (Fig. 4). The spectra of samples from weeks 4, 8, 12, and 16 were rather similar. The band at 1024 cm^{-1} was indicative of the aromatic C-H in-plane deformation. The strong band at 1219 cm^{-1} was caused by C-C, C-O, and C=O stretching. Syringyl (S) and condensed guaiacyl (G) absorptions were clearly observed at 1329 cm^{-1}, whereas guaiacyl ring breathing with C=O stretching appeared at 1373 cm^{-1}. The bands at 1420, 1503, and 1591 cm^{-1} corresponding to the aromatic skeletal vibrations,

and the C-H deformation combined with the aromatic ring vibration at 1462 cm^{-1} were present in these five spectra. The absorption at 1662 cm^{-1} was attributed to the carbonyl stretching in conjugated p-substituted aryl ketones. A wide absorption band at 3452 cm^{-1} originated from the OH stretching vibration in aromatic and aliphatic OH groups, whereas the bands at 2840, 2887, and 2937 cm^{-1} arose from the C-H asymmetric and symmetrical vibrations in the methyl and methylene groups, respectively. The lignin degraded by white-rot fungi revealed an intensity at the 1662 cm^{-1} band assigned to C=O in conjugated carbonyl groups, and untreated lignin showed this absorbance to a lesser extent. Moreover, a strong increasing intensity at the 1688 to 1708 cm^{-1} band was recorded in degraded lignin, which indicated unconjugated carbonyl groups. The results showed that during the bio-treatment of lignin, white-rot fungi generated conjugated and unconjugated C=O, which suggests that lignin biodegradation involved oxidation.

2D HSQC NMR Analysis of the Extracted Lignin

Two-dimensional ^{1}H-^{13}C NMR (2D NMR) provided important structural information and allowed for the resolution of otherwise overlapping resonances observed in either the ^{1}H or ^{13}C NMR spectra. To understand the detailed structural changes in the lignin fractions, they were characterized by 2D HSQC NMR. The HSQC NMR spectra of lignin showed two regions corresponding to the side chain (Fig. 5(a) and (b)) and aromatic ^{13}C-^{1}H correlations (Fig. 5(c) and (d)). The HSQC spectra of untreated wood lignin and treated lignin were similar, which meant that the main structure of lignin remained the same. In the side-chain regions of the HSQC spectra of these two lignin fractions, cross-signals of methoxyls (δC/δH 56.0/3.75) and side chains in β-O-4′ aryl ether linkages were the most prominent. The C_γ-H_γ correlations in β-O-4′ substructures were observed at δC/δH 72.1/4.85 (structures A, A′, and A″ (Fig. 6). The C_β-H_β correlations corresponding to the erythro and threo forms of the S-type β-O-4′ substructures were distinguished at δC/δH 86.0/4.10 and 86.0/3.98, respectively. These correlations shifted to δC/δH 83.9/4.29 in structure A linked to the G/H lignin units and γ-acylated β-O-4′ aryl ether substructures (A′ and A″) linked to the S lignin unit. The C_γ-H_γ correlations in structure A were observed at δC/δH 59.5 to 59.7/3.41 to 3.64. In addition to the β-O-4′ ether substructures, β-β′ (resinol, B) and β-5′ (phenylcoumaran, C) linkages were observed. Strong signals for resinol substructures B were observed with C_γ-H_γ, C_β-H_β, and the double C_γ-H_γ correlations at δC/δH 85.0/4.70, 53.8/3.09, and 71.1/4.19/3.84, respectively. Phenyl coumarin substructures C were found in lower amounts. The signals for their C_γ-H_γ and C_β-H_β correlations were discovered at δC/δH 87.0/5.49 and 53.1/3.47, respectively, whereas the C_γ-H_γ correlations overlapped with other signals at approximately δC/δH 62.5/3.73. In addition, C_γ-H_γ correlations (at δC/ δH 61.4/4.10) in the *p*-hydroxycinnamyl alcohol end group (I) and various signals from the associated carbohydrates and polysaccharide from fungi (δC/δH 65.0 to 77.1/2.9 to 4.2) were found in the side-chain regions of the lignin HSQC spectra.

In the aromatic regions of the HSQC spectra, cross-signals from the S- and G-lignin units were observed. The S-lignin units showed a prominent signal for the $C_{2,6}$-$H_{2,6}$ correlation at δC/δH 104.0/6.70, whereas the G units showed different correlations for C_2-H_2, C_5-H_5, and C_6-H_6 at δC/δH 111.1/6.99, 115.1/6.78, and 119.1/6.81, respectively. Signals corresponding to the $C_{2,6}$-$H_{2,6}$ correlations in C_α-oxidized S units (S′) (δC/δH 105.3/7.31) were present in all of the HSQC spectra of these two lignin fractions. The correlation for the C_2-H_2 in oxidized α-ketone structures G′ was observed in the spectra of MWL_0, and became stronger in the spectra of MWL_4. The $C_{2,6}$-$H_{2,6}$ correlations of PB were

observed as a strong signal at δC/δH 131.3/7.69. The signal at δC/δH 123.0/7.6 might be assigned to vanillic acid or its analogue (Huang *et al.* 1993; Ali *et al.* 2011), which was one of the lignin-degraded products (Fig. 7).

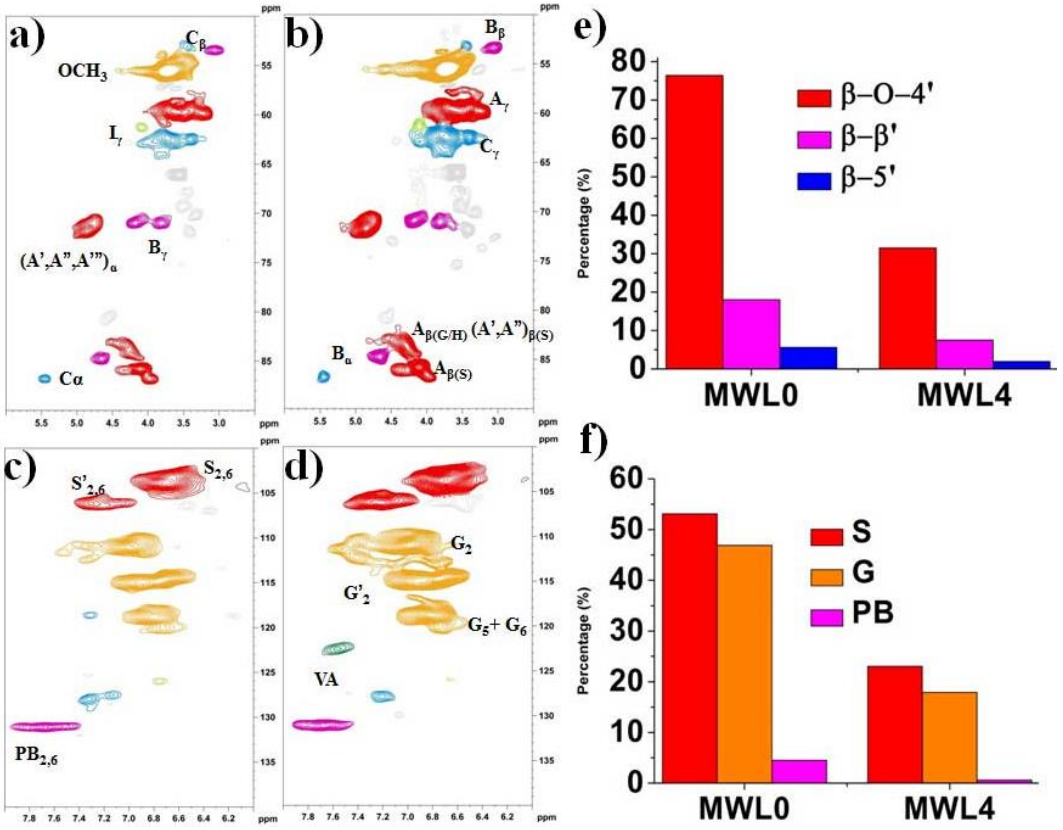

Fig. 5. 2D HSQC NMR spectra of the lignin fractions: a) side-chain regions of MWL0; b) aromatic regions of MWL0; c) side-chain regions of MWL4; d) aromatic regions of MWL4; e) changes in lignin side-chain linkage abundances, as percentage of total side-chains (calculated from the 2D-NMR spectra); f) percentage of lignin structural unit changes.

The different structural features among the treated and untreated lignin fractions were quantitatively investigated (Fig. 5(e) and (f)). The percentages of lignin side chains involved in the primary substructures A-C and the lignin units were calculated from the corresponding HSQC spectra (Wen *et al.* 2013). As expected, the main substructures present in all lignin fractions were the β-O-4′ linked ones (A, A′, and A″), which ranged from 31.5/100 Ar to 76.4/100 Ar. The β-β′ resinol substructure (B) appeared to be the secondary major substructure, comprising 7.5/100 Ar to 18.0/100 Ar. The phenylcoumaran substructures (C) were calculated to be minor amounts, ranging from 1.9/100 Ar to 5.6/100 Ar. The content of β-O-4′ aryl ether in MWL_0 was 76.4/100Ar, and it decreased to 31.5/100 Ar in MWL_4. These data suggested that the cleavage of the β-O-4′ aryl ether (depolymerization) is the predominant reaction during bio-treatment. This might be because of the high activity of LiP in *T. pubescens* C7571, which attacks the β-O-4′ linkage of lignin (Umezawa *et al.* 1987). In addition to β-O-4′ aryl ether linkage cleavage and carbon-carbon linkage degradation, the S/G ratio in lignin was another prominent structural alteration observed after bio-treatment. The S, G, and PB ratios decreased from 53.1/100 Ar, 46.9/100 Ar, and 4.5/100 Ar to 23.0/100 Ar, 17.9/100 Ar, and 0.6/100 Ar for MWL_0

and MWL_4, respectively. Interestingly, the data also suggested that the G-type lignin was further degraded than the S-type, as revealed by a slightly elevated S/G ratio in MWL_0 (1.13) and MWL_0 (1.29). Thus, G-type lignin was more easily degraded. Another possible reason is that the isolated MWL was mainly extracted from the middle lamella of the cell wall (Whiting and Goring 1982), which is more easily penetrated by the hyphae of white-rot fungi. Because G-type lignin has less methoxyl than S-type lignin, the cross-signals of methoxyls (δC/δH 56.0/3.75) of MWL_4 were stronger.

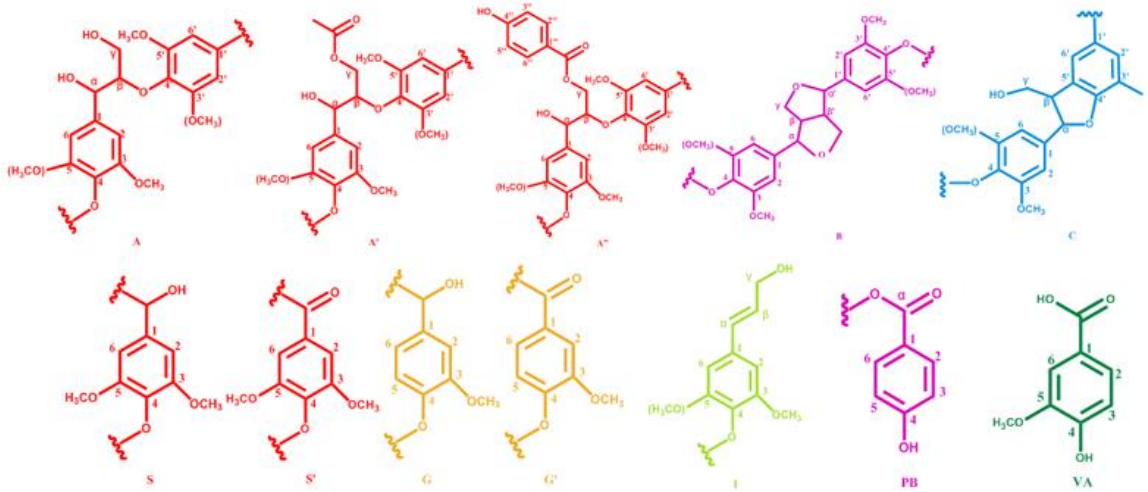

Fig. 6. Main substructures of lignin involving different side-chain linkages and aromatic units identified by HSQC: (A) β-O-4′ aryl ether linkages with a free –OH at the γ carbon; (A′) β-O-4′ linkages with a carbonyl group at Cγ; (A″) β-O-4′ linkages with p-hydroxybenzoated –OH at Cγ; (B) resinol structures formed by β-β′/α-O-γ′/γ-O-α′linkages; (C) phenylcoumaran structures formed by β-5′/α-O-4′ linkages; (G) guaiacyl unit; (G′) oxidized guaiacyl unit with an α-ketone; (S) syringyl unit; (S′) oxidized syringyl unit with a carbonyl group at Cα (phenolic); (I) p-hydroxy-cinnamyl alcohol end group; (PB) p-hydroxybenzoate substructures; (VA) vanillic acid or its analogue

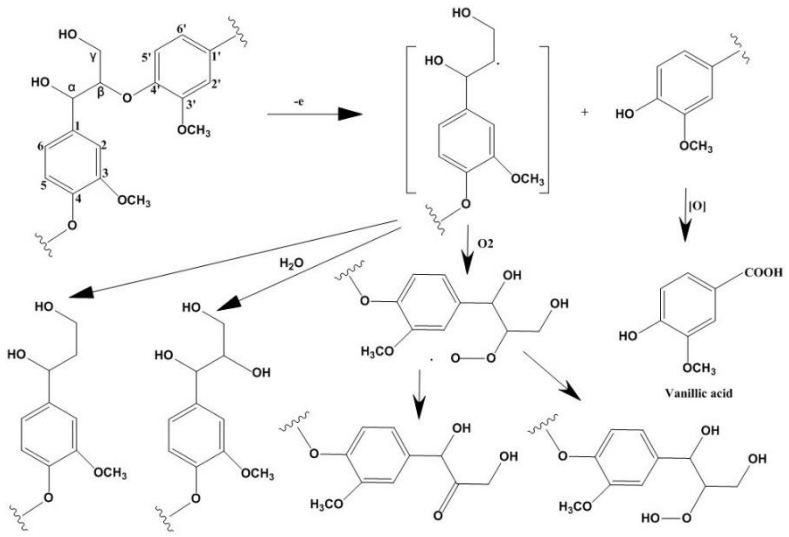

Fig. 7. Possible lignin degradation processes

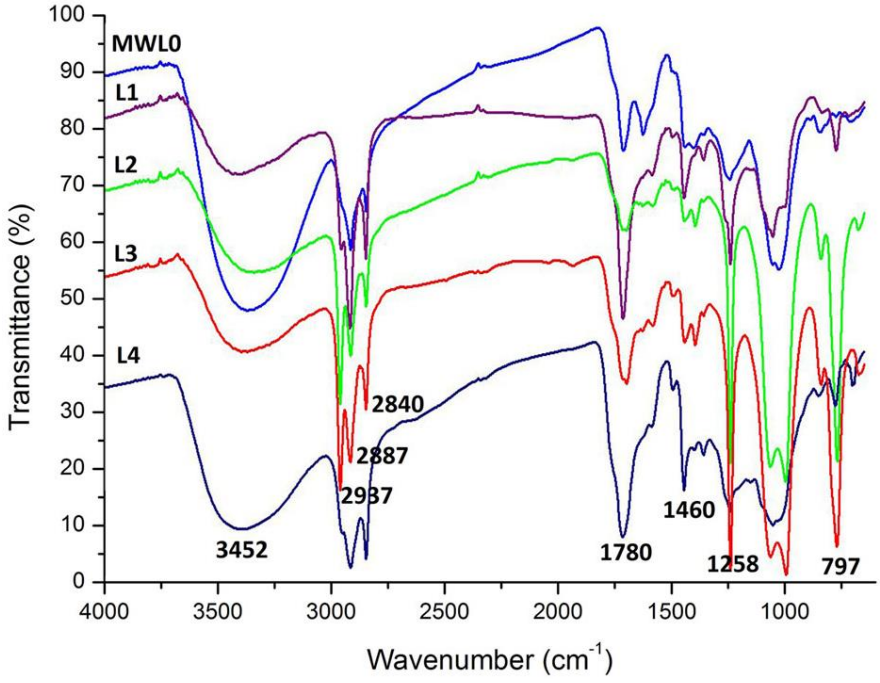

Fig. 8. FT-IR spectra of the lignin degradation products

FT-IR Analysis of the Extracted Lignin

To identify the chemical groups of the degradation compounds formed during white-rot fungi treatment, the degradation products were analyzed using FT-IR spectroscopy. The wide absorption band at 3452 cm^{-1} originated from the OH stretching vibration in aromatic and aliphatic OH groups, whereas the bands at 2937, 2887, and 2840 cm^{-1} were attributed to the C-H asymmetric and symmetrical vibrations in the methyl and methylene groups, respectively. The absorption band at 1708 cm^{-1} was attributed to the C=O in the conjugated carbonyl groups, and the absorption band at 1658 cm^{-1} was attributed to the α-C=O. The bands at 1460 cm^{-1}, corresponding to aromatic skeletal vibrations and the C-H deformation, combined with aromatic ring vibration at 1459 cm^{-1}, were present in these four spectra of lignin degradation products. The strong band at 1258 cm^{-1} was caused by the C-C, C-O, and C=O stretching of the syringyl units. The bands at 1085 (1011) cm^{-1} and 797 cm^{-1} were attributed to the polysaccharides of white-rot fungi and hexose. As shown in Fig. 8, high amounts of conjugated and unconjugated C=O functionalities were shown in the spectra of lignin degradation products. Similar results were observed in *T. versicolor* treated beech wood that unconjugated C=O functionalities increased after fungi treatment (Bari *et al.* 2015). The FT-IR spectra of lignin degradation products revealed that side chain oxidation was one of the main reactions that occurred during bio-treatment, which was also observed by the aforementioned 2D-HSQC analysis.

GC-MS Analysis of the Lignin Degradation Compounds

Gas chromatography/mass spectrometry (GC-MS) is a convenient tool for the rapid analysis of lignin, and it has been used to characterize different patterns of wood decay by fungi. To obtain more detailed insight into the degradation of lignin during fungal decay, lignin degradation products were subjected to Py-GC/MS analysis. The complete series of Py-GC/MS compounds identified in the degradation products are included in Table 3 and Fig. 9.

According to the chemical structure, the degradation products were divided into five categories: aldehydes, phenols, organic acids, alkanes, and benzenes. In both degraded samples (L_2 and L_4), debris from S- and G-type units were observed. The two peaks at 11.2 (3,5-dimethyl-benzaldehyde) and 15.6 (2,4-bis(1,1-dimethylethyl) phenol) most likely originated in the S units, whereas the peaks at 12.4 (4-methoxy-benzaldehyde) and 14.4 (vanillin) were attributed to the degradation of the G-type units in lignin. Specifically, vanillin (peak 2, Fig. 9), an important degradation product, was also found in the 2D NMR. Simultaneously, a small increase in the abundance of 1,2-benzenedicarboxylic acid (peak 14, Fig. 9) and other organic acids (peak 4, 13, 15, 16, and 18) were observed, confirming that some oxidative alteration of the lignin side-chains (β-O-4′, β-β′, and β-5′) occurred during white-rot decay, as shown by FT-IR and 2D HSQC NMR. Furthermore, the high abundance of alkanes released upon Py-GC/MS analysis indicates that a ring-opening reaction occurred in the white-rotted wood, and the alkyl chain length was between 12 and 27.

The other benzene-type compounds, including benzene propanol (peak 7), 2-(methylthio)-benzothiazole (peak 11), 1,6-dimethyl-4-(1-methylethyl)-naphthalene (peak 12), 1,2-benzenedicarboxylic acid (peak 14), 3-methyl-n,n-bis(3-methylphenyl)-benzenamine (peak 19), dioctyl phthalate (peak 21), and 1-nitro-2-(1,1,2,2-tetrafluoroethoxy)-benzene (peak 22) may be the derivatives of degradation products. These results confirmed the oxidative alteration of lignin side-chains by the detection of debris from units.

Table 3. Py-GC/MS Analysis of Lignin Degradation Compounds

No. [a]	Variety	RT [b]	Compounds
1	Aldehydes	11.2	3,5-dimethyl-benzaldehyde
2		14.4	Vanillin
8		12.4	4-methoxy-benzaldehyde
3/17/20	Phenols	15.6	2,4-bis(1,1-dimethylethyl) phenol
4	Organic acids	17.2	Oxalic acid
13		18.23	Fumaric acid
15		21.5/26.3	Succinic anhydride
16		22.3	9,12-octadecadienoic acid
18		26.6	1-phenanthrene carboxylic acid
5	Alkanes	22.8	Heptacosane
6		11.4	Dodecane
9		16.2	Octadecane
10		16.3	Tetracosane
7	Benzenes	12.1	Benzene propanol
11		16.9	2-(methylthio)-benzothiazole
12		18.2	1,6-dimethyl-4-(1-methylethyl)-naphthalene
14		19.7	1,2-benzenedicarboxylic acid
19		26.1	3-methyl-N,N-bis(3-methylphenyl)-benzenamine
21		26.7	Dioctyl phthalate
22		27.0	1-nitro-2-(1,1,2,2-tetrafluoroethoxy)-benzene

[a] NO. represents peaks labeled in Fig. 9
[b] RT, reaction time

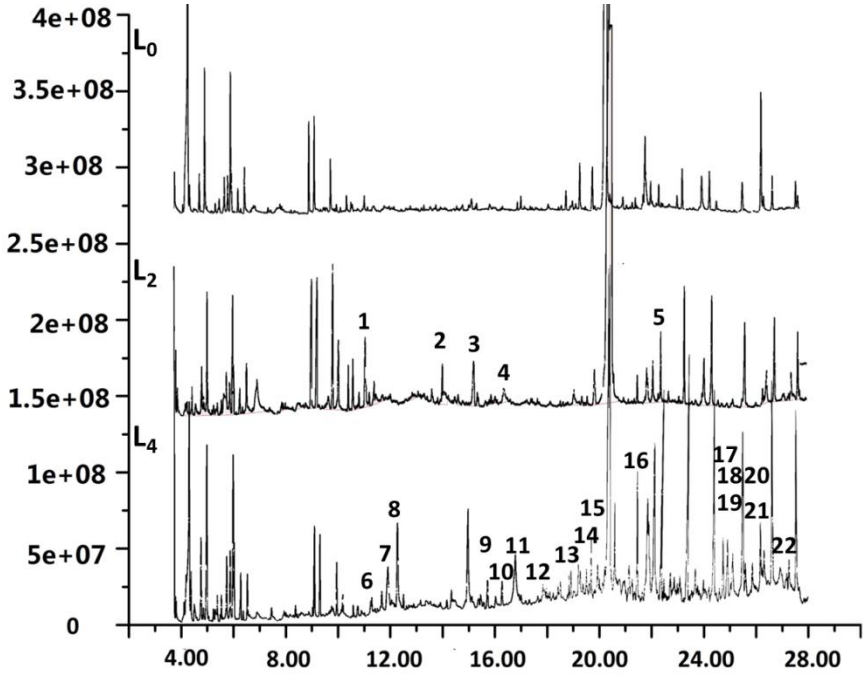

Fig. 9. Py-GC/MS analysis of lignin degradation products

CONCLUSIONS

1. *T. pubescens* C7571 showed higher enzyme activity (particularly LiP) than *T. versicolor* C6915, thus giving a low lignin content of 10.4%. The cleavage of β-O-4′ aryl ether was the predominant reaction, which may be caused by the high activity of LiP.
2. The decrease in lignin molecular weights suggested fragmentation reactions, which was further confirmed by FT-IR spectroscopy. G-type lignin was more easily degraded than S-type lignin, and the degradation products of the G units (*e.g.*, vanillin) were found by 2D HSQC NMR and GC-MS analyses.
3. The study of lignin alterations during white-rot fungi treatment could be beneficial for the sustainable production of chemicals, materials, and fuels from renewable plant resources.

ACKNOWLEDGMENTS

This work was supported by Fundamental Research Funds for the Central Universities (No. BLYJ201512), the National Science Fund for Distinguished Young Scholars (31225005), and the Chinese Ministry of Education (113014A).

REFERENCES CITED

Ali, K., Maltese, F., Fortes, A. M., Pais, M. S., Choi, Y. H., and Verpoorte, R. (2011). "Monitoring biochemical changes during grape berry development in Portuguese

cultivars by NMR spectroscopy," *Food Chem.* 124(4), 1760-1769. DOI: 10.1016/j.foodchem.2010.08.015

Arora, D. S., and Sharma, R. K. (2010). "Ligninolytic fungal laccases and their biotechnological applications," *Appl. Biochem. Biotech*. 160(6), 1760-1788. DOI: 10.1007/s12010-009-8676-y

Bari, E., Nazarnezhad, N., Kazemi, S. M., Ghanbary, M.A.T., Mohebby, B., Schmidt, O., and Clausen, C.A. (2015). "Comparison between degradation capabilities of the white rot fungi *Pleurotus ostreatus* and *Trametes versicolor* in beech wood," *Int. Biodeter. Biodegr.* 104, 231-237. DOI: 10.1016/j.ibiod.2015.03.033

Björkman, A. (1954). "Isolation of lignin from finely divided wood with neutral solvents," *Nature* 174, 1057-1058. DOI: 10.1038/1741057a0

Bozell, J. J., O'Lenick, C. J., and Stacy, W. (2011). "Biomass fractionation for the biorefinery: Heteronuclear multiple quantum coherence–nuclear magnetic resonance investigation of lignin isolated from solvent fractionation of switchgrass," *J. Agr. Food Chem.* 59(17), 9232-9242. DOI: 10.1021/jf201850b

Dias, A. A., Bezerra, R. M., and Pereira, A. N. (2004). "Activity and elution profile of laccase during biological decolorization and dephenolization of olive mill wastewater," *Bioresour. Technol.* 92(1), 7-13. DOI: 10.1016/j.biortech.2003.08.006

Dinis, M. J., Bezerra, R. M. F., Nunes, F., Dias, A. A., Guedes, C. V., Ferreira, L. M. M., Cone, J. W., Marques, G. S. M., Barros, A., and Rodrigues, M. A. M. (2009). "Modification of wheat straw lignin by solid state fermentation with white-rot fungi," *Bioresour. Technol.* 100, 4829-4835. DOI: 10.1016/j.biortech.2009.04.036

Elegir, G., Daina, S., Zoia, L., Bestetti, G., and Orlandi, M. (2005). "Laccase mediator system: Oxidation of recalcitrant lignin model structures present in residual kraft lignin," *Enzyme Microb. Tech.* 37(3), 340-346. DOI: 10.1016/j.enzmictec.2005.02.017

Ghose, T. K., and Bisaria, V. S. (1987). "Measurement of hemicellulase activities. Part 1: xylanases," *Pure Appl. Chem.* 59(12), 1739-1752. DOI: 10.1351/pac198759121739

Heinfling, A., Ruiz-Dueñas, F. J., Martínez, M. J., Bergbauer, M., Szewzyk, U., and Martínez, A. T. (1998). "A study on reducing substrates of manganese-oxidizing peroxidases from *Pleurotus eryngii* and *Bjerkandera adusta*," *Febs Lett.* 428(3), 141-146. DOI: 10.1016/S0014-5793(98)00512-2

Hofrichter, M. (2002). "Review: Lignin conversion by manganese peroxidase (MnP)," *Enzyme Microb. Tech.* 30(4), 454-466. DOI: 10.1016/S0141-0229(01)00528-2

Huang, Z., Dostal, L., and Rosazza, J. P. (1993). "Mechanisms of ferulic acid conversions to vanillic acid and guaiacol by *Rhodotorula rubra*," *J. Biol. Chem.* 268(32), 23954-23958.

Kapich, A. N., Prior, B. A., Lundell, T., and Hatakka, A. (2005). "A rapid method to quantify pro-oxidant activity in cultures of wood-decaying white-rot fungi," *J. Microbiol. Meth.* 61, 261-271. DOI: 10.1016/j.mimet.2004.12.010

Kuhar, F., Castiglia, V., and Levin, L. (2015). "Enhancement of laccase production and malachite green decolorization by co-culturing *Ganoderma lucidum* and *Trametes versicolor* in solid-state fermentation," *Int. Biodeter. Biodegr.* 104, 238-243. DOI: 10.1016/j.ibiod.2015.06.017

Mao, J. Z., Zhang, X., Li, M. F., and Xu, F. (2013). "Effect of biological pretreatment with white-rot fungus *Trametes hirsuta* C7784 on lignin structure in *Carex meyeriana* Kunth," *BioResources* 8(3), 3869-3883. DOI: 10.15376/biores.8.3.3869-3883

Martínez Ferrer, Á. T., Rencoret, J., Nieto Garrido, L., Jiménez-Barbero, J., Gutiérrez

Suárez, A., and Río Andrade, J. C. (2011). "Selective lignin and polysaccharide removal in natural fungal decay of wood as evidenced by *in situ* structural analysis," *Environ. Microbiol.* 13(1), 96-107. DOI: 10.1111/j.1462-2920.2010.02312.x

Mate, D. M., Garcia-Ruiz, E., Camarero, S., Shubin, V. V., Falk, M., Shleev, S., Ballesteros, A. O., and Alcalde, M. (2013). "Switching from blue to yellow: Altering the spectral properties of a high redox potential laccase by directed evolution," *Biocatal. Biotransfor.* 31(1), 8-21. DOI: 10.3109/10242422.2012.749463

Miller, G. L. (1959). "Use of dinitrosalicylic acid reagent for determination of reducing sugar," *Anal. Chem.* 31(3), 426-428. DOI: 10.1021/ac60147a030

Souza-Cruz, P. B. D., Freer, J., Siika-Aho, M., and Ferraz, A. (2004). "Extraction and determination of enzymes produced by *Ceriporiopsis subvermispora* during biopulping of *Pinus taeda* wood chips," *Enzyme Microb. Tech.* 34(3–4), 228-234. DOI: 10.1016/j.enzmictec.2003.10.005

Tien, M., and Kirk, T. K. (1988). "Lignin peroxidase of *Phanerochaete chrysosporium*," *Method Enzymol.* 161, 238-249. DOI: 10.1016/0076-6879(88)61025-1

Umezawa, T., and Higuchi, T. (1987). "Mechanism of aromatic ring cleavage of β-O-4 lignin substructure models by lignin peroxidase," *Febs Lett.* 218(2), 255-260. DOI: 10.1016/0014-5793(87)81057-8

Wen, J. L., Yuan, T. Q., Sun, S. L., Xu, F., and Sun, R. C. (2013). "Understanding the chemical transformations of lignin during ionic liquid pretreatment," *Green Chem.* 16(1), 181-190. DOI: 10.1039/c3gc41752b

Wen, J. L., Sun, S. L., Yuan, T. Q., and Sun, R. C. (2014). "Structural elucidation of whole lignin from Eucalyptus based on preswelling and enzymatic hydrolysis," *Green Chem*. 17(3),1589-1596. DOI: 10.1039/c4gc01889c

Whiting, P., and Goring, D. A. I. (1982). "Chemical characterization of tissue fractions from the middle lamella and secondary wall of black spruce tracheids," *Wood Sci. Technol.* 16(4), 261-267. DOI: 10.1007/BF00353149

Wörmeyer, K., Ingram, T., Saake, B., Brunner, G., and Smirnova, I. (2011). "Comparison of different pretreatment methods for lignocellulosic materials. Part II: Influence of pretreatment on the properties of rye straw lignin," *Bioresource Technol.* 102(5), 4157-4164. DOI: 10.1016/j.biortech.2010.11.063

Yelle, D. J., Wei, D., Ralph, J., and Hammel, K. E. (2011). "Multidimensional NMR analysis reveals truncated lignin structures in wood decayed by the brown rot basidiomycete *Postia placenta*," *Environ. Microbiol.* 13(4), 1091-1100. DOI: 10.1111/j.1462-2920.2010.02417.x

Zadrazil, F. (1985). "Screening of fungi for lignin decomposition and conversion of straw into feed," *Angew. Bot.* 59, 252-433. DOI: 10.1007/BF02826558

Zhao, Q., and Dixon, R. A. (2011). "Transcriptional networks for lignin biosynthesis: More complex than we thought," *Trends Plant Sci.* 16(4), 227-233. DOI: 10.1016/j.tplants.2010.12.005

Article submitted: January 8, 2016; Peer review completed: February 12, 2016; Revised version received and accepted: February 28, 2016; Published: March 14, 2016.
DOI: 10.15376/biores.11.2.3972-3986